NASA Technical Memorandum 110179

NASA-TM-110179 19950023830

Emissivity Measurements in Thin Metallized Membrane Reflectors Used for Microwave Radiometer Sensors

L. C. Schroeder, R. L. Cravey, M. J. Scherner, C. P. Hearn, and H.-J. C. Blume
Langley Research Center, Hampton, Virginia

June 1995

National Aeronautics and
Space Administration
Langley Research Center
Hampton, Virginia 23681-0001

I. Introduction

This paper is concerned with electromagnetic losses in metallized films used for inflatable reflectors. The issue arose in NASA reviews of the planned INSTEP flight experiment, the Inflatable Antenna Experiment (IAE), manifested for 1996 shuttle flight to demonstrate this technology (ref. 1). An inflatable membrane is made of tough elastic material such as Kapton, and it is not electromagnetically reflective by design. A film of conducting metal is added to the membrane to enhance its reflective properties. Since the impetus for use of inflatables for spacecraft is the light weight and compact packaging, it is important that the metal film be as thin as possible. However, if the material is not conductive or thick enough, the radiation due to the emissivity of the reflector could be a significant part of the radiation gathered by the radiometer. The emissivity would be of little consequence to a radar or solar collector; but for a radiometer whose signal is composed of thermal radiation, this contribution could be severe. For example, the Space Sensor Microwave/Imager microwave radiometer currently in space requires reflector emissivities of less than .002 (ref. 2) to obviate the need for thermal correction of its data.

Bulk properties of the metal film cannot be used to predict its loss. For this reason, a program of analysis and measurement was undertaken to determine the loss behavior of a number of candidate metallized film reflectors. For discussion of the analysis as well as the theoretical basis of thin film conductivity, see reference 3. The samples chosen for study are described in the next section. Measurements were made using (1) a network analyzer system with an L-band waveguide, (2) an S-band radiometer, and (3) a network

analyzer system with a C-band antenna free-space transmission system. These measurement techniques will be reviewed in Section III. A set of tests to directly measure sample thickness and quality were also performed. These tests will be described in Section IV. In Section V, the experimental results of the program are presented. Section VI contains the conclusions drawn during the measurement program.

II. Sample Description

The selection of samples of metallized reflector membranes was a joint effort by NASA Langley researchers, JPL IAE program management, and L'Garde. The set of samples chosen was purchased by L'Garde from industrial suppliers using funds supplied by NASA Langley.

The substrate material chosen for the samples was .3 mil thick Kapton, onto which a nominal thickness of gold, silver, or aluminum was sputtered or vapor deposited. Various thicknesses of the metals were specified in an attempt to provide a range of samples, some of which were highly reflective (3000 Å) while others were quite lossy (100 Å). Table 1 shows the matrix of samples provided. The sample selection allows for comparison of different thicknesses of the same metal and for comparison of different metals at the same thickness.

III. Measurement Systems

1. Waveguide System

The waveguide measurements of the thin metallized membranes are performed using an HP 8510C network analyzer to measure reflection from and transmission through the membranes. Measurements have been performed at L-band (1.12 - 1.8 GHz) frequencies and are planned for S-band (2.6 - 3.95 GHz). The L-band frequency range was chosen due to the fact that this is the selected operational frequency for the radiometer (soil moisture) application. Since the S-band frequency range overlaps the frequencies of the other two available measurement techniques, these measurements are planned for comparison purposes. From the reflection and transmission measurements, emissivity is computed as a function of frequency across the waveguide band. The emissivity at each frequency is assumed to be equal to the difference between the incident power ratio and the sum of the reflected and transmitted power ratios:

$$e = 1 - \left(S_{11}^{\,2} + S_{21}^{\,2}\right) \qquad (1)$$

a. Measurement setup and calibration

The waveguide setup for L-band is illustrated in figure 1. As can be seen from the figure, the fixture includes two 7 mm coaxial to L-band waveguide transitions, two straight pieces of L-band waveguide, and the waveguide flange which supports the sample. A full two-port calibration is performed to the reference planes at the ends of the straight pieces of waveguide. These pieces are included to assure that unwanted modes excited by the coaxial-to-waveguide transition are damped out before reaching the material under test. The full two-port calibration involves measuring waveguide standards

consisting of a short at the measurement plane, a short offset from the measurement plane, a matched load, and a through connection in which the two straight pieces of waveguide are directly connected.

The membrane samples are mounted on the waveguide flanges as shown in figure 2. To mount the samples, the metallized side of each sample is attached to one side of the flange which has been coated with a spray adhesive. The material extending beyond the flange is then trimmed, and the flange is wrapped in copper tape to provide sufficient conductivity when the flange is placed between the waveguide extensions for the measurement. Before the samples are mounted, each empty flange is characterized in the measurement setup in order to assure that the response from the sample holder is small enough not to affect the measurement.

b. Measurement Characterization

Measurement of the reflection and transmission properties of the metallized membrane samples in the waveguide setups provides some advantages over the other measurements, including providing a fairly quick, repeatable method for estimation of the emissivity. The waveguide measurements are done at room temperature and do not require a cold load as does the radiometer setup, and the waveguide setup does not require a large amount of space as does the free space method. Also, a concern in comparing the measurement of emissivity using the radiometer system and the transmission measurement using the free space system is that the two systems operate at different frequencies. The S-band waveguide frequency range overlaps both the other two systems, and planned S-band waveguide measurements will make at least one comparison for each system at the same

frequency possible. The waveguide system also has some drawbacks. The waveguide setup does not provide a direct measurement of the emissivity as does the radiometer system. Also, the incident wave is not normal to the membrane sample, and for highly reflective samples it is difficult to obtain an accurate measurement of S_{11}. These drawbacks are overcome in the free space measurement scheme, with the use of the focused antenna system and the fact that only a transmission measurement is needed to compute emissivity in that case.

2. Radiometric System

S-band radiometer emissivity measurements are performed at 2.65 GHz for the metallized foil samples described earlier. Measurements are based upon the basic law of physics that all objects at temperatures above absolute zero radiate energy in the form of electromagnetic waves. By using the Raleigh-Jeans approximation, the radiation emitted by a given sample is directly proportional to its emissivity. The S-band radiometer measurement system (ref. 4) consists of a radiometer (2.65 GHz) connected to a horn antenna, a test chamber attached to the end of the antenna, and a cryogenic matched load radiating toward the sample under test inside the chamber as shown in figure 3.

The radiometrically measured brightness temperature consists of the sample's internal emission and the emission of the cryogenic load, reflected from the sample. The sample's emission varies with physical temperature while the load's emission is considered constant through the measurement period. By changing the chamber temperature from T_{M1} to T_{M2}, the radiometer measures the brightness temperature T_{B1} to T_{B2}, respectively. If the sample temperature

and chamber temperature are assumed to be equivalent, the surface emissivity of the sample can be written as:

$$e = \frac{T_{B2} - T_{B1}}{T_{M2} - T_{M1}} \qquad (2)$$

a. Preliminary Chamber Temperature Surveys

In the preliminary studies, attention was given to understanding the temperature distribution within the chamber without test samples mounted. Fifteen platinum resistance temperature detectors (RTDs) were equally spaced within the chamber near the heating plate, and two RTDs were placed within the outlet air tubes and used to measure the temperature distribution in the chamber. As a result of these studies, the air inlet and outlet holes in the chamber were enlarged and a second heater was added to the chamber's manifold to insure a uniform distribution within the empty chamber. A uniform distribution in the empty chamber would help guarantee that the test sample would not experience any temperature gradients during the measurement period. Temperature distribution tests were then made with samples mounted within the chamber. Under ambient conditions, the 15 RTDs had a standard deviation of .14°C. When the chamber was heated and a maximum temperature of 59°C was achieved, the standard deviation was .93°C. The 15 RTDs were then removed so that they would not interfere with the radiometric measurement, and the two outside RTDs were used to extrapolate the chamber's temperature.

b. Test Procedures and Data Analysis

A measurement period started with measuring the sample and brightness temperatures at room temperature from time t = 0 seconds to approximately

t = 550 seconds (fig. 4, 100 Å aluminum sputtered sample as an example). During this interval, the average sample physical and brightness temperatures, T_{M1} and T_{B1} respectively, were calculated. Heaters in the chamber were then turned on at t = 550 seconds and turned off at t = 1750 seconds. Between t = 1600 seconds and t = 1750 seconds, the sample achieved its maximum physical temperature and the average sample physical and brightness temperatures, T_{M2} and T_{B2} respectively, were calculated. Averaging was done over a 50 second interval during the t = 0 to 550 seconds and the t = 1600 to 1750 seconds periods at a rate of one measurement every 5 seconds. With T_{M1}, T_{M2}, T_{B1}, and T_{B2}, each an average of ten measurements, the emissivity and loss were determined from (2) and (3).

The average emissivity and standard deviation was calculated from several tests for each sample. As an example, Table 2 gives the results for the 650 Å gold sputtered sample. Three tests were excluded from the average emissivity calculation because the radiometer became unstable during these tests; this was due to either the varying liquid nitrogen level in the cryogenic load or interference received by external sources of radiation. Similar measurements were made for the other samples.

3. Free-Space Transmission System

This section describes the application of a vector network analyzer (VNA) to "free-space" measurements of the electromagnetic properties of the metallized thin membranes described in Section II. The Kapton sheets alone are essentially transparent to the EM wave and the conducting films are all much less than one skin-depth thick at 7.2 GHz, the highest test frequency.

a. Measurement Approach

The approach described here began with a recognition that (a) the worst-case measurement error associated with measuring the "free-space" reflectivity, Γ, of these materials with a VNA would probably be as large, or larger, than the loss and transmission factors, (b) transmission can generally be measured to a higher degree of accuracy than reflection, and (c) the thinness of the samples allowed them to be modeled as simple lossy, lumped zero-length elements in the free-space transmission path.

The "free-space transmission" test fixture shown in figure 5 consists of 18 inch diameter dishes fed with WR-187 waveguide horns pointed at each other. A 6 x 6 ft vertical "isolating wall" covered on both sides with EM absorber and having a 1 x 1 ft square "sample aperture" is located between the dishes. The dishes are connected to an HP 8720C VNA with precision coaxial cables.

The VNA is operated in a two-port, "time-domain" mode spanning 3.8-7.2 GHz (this exceeds the normal operating range of WR-187 waveguide, which is 3.95 to 5.85 GHz), allowing the use of "time gating" to reduce spurious responses caused by system non-idealities: leakage and multiple reflections. Microwave absorbing materials are used judiciously to squelch leakage and reduce internal reflections (the worst internal reflection was caused by the feed-horn mounting brackets). The time gate is set to pass only the response corresponding to the direct path through the test aperture. Responses outside the time gate are effectively eliminated.

Figure 6 is an idealized model of the test configuration: a transmission line having a zero-length shunt admittance, Y, at the measurement plane.

Deviations from that model in the actual test system are largely accounted for by proper calibration. Ultimately, this measurement is based on the ratio of measurements made with the sample inserted to those with the aperture open.

A relationship between S_{21}, the forward transmission coefficient measured between the input and output ports of the test fixture, and the shunt admittance, Y, can be developed from elementary transmission line theory. The fraction of the incident wave, V_F, which arrives at the measurement plane is $V_F \cdot L_1$. The measurement plane termination, $Y_T = Y + Y_O$, produces a reflection coefficient given by:

$$\Gamma = -(Y_T - Y_O)/(Y_T + Y_O) = -Y/(Y + 2Y_O) \tag{3}$$

The net voltage across Y is the sum of the forward and reflected waves at X = 0 and constitutes the remaining forward-traveling wave at $X = 0^+$

$$V_T = (1 + \Gamma)\, V_F \cdot L_1 \tag{4}$$

Combining equations (3) and (4) gives

$$V_T = V_F \cdot L_1 (2Y_O)/(Y + 2Y_O) \tag{5}$$

This wave propagates towards the load and is attenuated by the factor L_2 before being absorbed by the matched termination, Y_L. The measured forward transmission coefficient of the entire system is therefore:

$$S_{21} = V_L/V_F = L_1 \cdot 2Y_O/(Y + 2Y_O)L_2 \tag{6}$$

With the aperture open, Y = 0, and

$$[S_{21}]_{OPEN} = [S_{21}]_T = L_1 \cdot L_2 \tag{7}$$

The ratio

$$S_{21}/[S_{21}]_{OPEN} = 2Y_O/(Y + 2Y_O) \tag{8}$$

can be solved directly for the equivalent shunt admittance, Y at X = 0. The reflection (Γ) and transmission (T) coefficients at the measurement plane, X = 0, can be computed after Y is determined from equation (8); Γ from equation (3) and T from

$$T = 1 + \Gamma \tag{9}$$

The emissivity-absorption loss of the material can be found from the power relationship that must be satisfied at the measurement plane:

$$P_{INCIDENT}\big|_{x=o} = P_{REFL}\big|_{x=o} + P_{DISS}\big|_{x=o} + P_{TRAN}\big|_{x=o} \tag{10}$$

The emissivity when the material is in thermal equilibrium is found from equation 10 as:

$$e \equiv P_{DISS}\big|_{X=O} / P_{INC}\big|_{X=O} = 1 - |\Gamma|^2 - |T|^2 \tag{11}$$

b. Calibration and Error Correction

The calibration scheme options for this two-port free-space measurement were TRL, LRM, and Response [ref. 5]. The TRL calibration requires a "Through", a "Reflect" (of essentially zero thickness having zero transmission) at the measurement plane, and a "Line" (a finite length of transmission line). The LRM calibration requires a "Line," with the aperture open, a "Reflect" and a "Match," with the opening filled with absorber. The test fixture configuration used here is such that an LRM calibration would be preferred to a TRL calibration, since the LRM does not necessitate physically moving the antennas to change the electrical path length [ref. 4].

Since only S_{21} is needed, a much simpler response-isolation calibration procedure was used which is believed to be inherently superior to a conventional LRM calibration. The advantage of this technique is the absence

of residual (post-calibration) source and load-match discontinuities at the measurement plane. A vector subtraction of that portion of the measured S_{21} response due to signal paths other than the primary, direct path through $[S_{21}]_{open}$. This step enhances the isolation achieved by the wall of absorber and reduces spurious signals having path delays falling within the time gate - which would not be reduced by the time gate. This "correction" vector is found by measuring S_{21} with a plate in the sample aperture having the same dimensions as the test samples, which is denoted as $[S_{21}]_R$. If vector-error subtraction is used to improve the isolation, the forward transmission coefficient after vector subtraction,

$$[S_{21}]_{TRUE} = [S_{21}]_{MEASURED} - [S_{21}]_R \qquad (13)$$

should be used in equation (8).

c. System Accuracy

There has not yet been a serious attempt to conduct an extensive error analysis of this technique. Such an analysis may be extremely difficult. However, an attempt was made in the conceptual phase of development to identify and reduce obvious error sources, as discussed above. Concerns about the effect of the measurement plane being within the far-field region of the antennas (usually defined as $2D^2/\lambda$; 17.3 ft at 3.8 GHz and 33 ft at 7.2 GHz) and the resulting spherical nature of the wavefront inpinging upon the test material have been approached experimentally. Calibrations and measurements made with several antenna spacings produced essentially identical results. A more complete parametric study is planned to further evaluate the effect of antenna spacing on the $[S_{21}]_{TRUE}$ measurement.

IV. Sample Quality Measurements

During the course of this study, concerns were raised about the metal layer thicknesses for some of the samples. For this reason, an investigation into the quality of the samples was undertaken. These sample quality measurements are described in the following subsections.

1. **Microscopic Photos.** These photos were taken in the Photonics Laboratory at NASA Langley using a Stereo MicroZoom II microscope, which was attached to a digital camera. A scale which displays 10 microns is shown on each picture. These photos were the first observations of metal layer quality. From these photos, it was hypothesized that the deposited surfaces were inhomogeneous (see the large cells which appear in the photographs, figs. 7 and 8). It seemed that the cells might indicate that the materials were being deposited in large blobs, which could adversely affect the conductivity of the finished thin film.

2. **Surface Resistivity.** Surface resistivity measurements were performed on the metallized films at L'Garde for unfolded, folded, and crumpled samples before the samples were sent to NASA Langley. These measurements were repeated for unfolded samples at NASA Langley, using a four-probe array fixture which was made according to L'Garde specifications (ref. 6), along with a Fluke 8842A Multimeter. The measurement involved bringing a 1 inch wide strip of test material in contact with the probe across the four probe legs (see fig. 9) and then recording the resistivity in ohms/square as read from the multimeter. To assure good contact, the test material was pressed onto the surface of the probe using a weighted plexiglass plate lined with a piece of insulating flexible foam material. The strips of material were approximately

8 inches long, and several measurements were taken along the length of the material in order to account for possible variations in material thickness and resistivity. Several known resistivity materials were measured before the thin metallized membrane samples to test the procedure and apparatus.

Results of these measurements were compared to the surface resistivity measurements made by L'Garde. For most materials, the average resistivity measured by L'Garde and by NASA agreed within 10 percent. The results for unfolded samples from L'Garde and NASA Langley are summarized in Tables 3 (ref. 5) and 4. Note that the values for the vapor deposited aluminum had large percent difference values, suggesting that the thickness of the material varied quite a bit along the length of the strip.

3. **Scanning Transmission Electron Microscope (STEM) Pictures.** These studies were performed by the Virginia Institute of Marine Science under NASA Langley contract to Anne St. Clair of the Materials Division. These studies allowed determination of the thicknesses of both the Kapton substrate and the metal deposition layer (see figs. 10 and 11). From the results of the selected sputtered samples (see Table 5) it was determined that the "average" (determined by a rough measurement with a scale) thicknesses of samples were within $\pm$25 percent of the intended values, at least for the small portion of the sample that was viewed using this technique. As can be seen from the pictures, however, for some materials, the thickness of the metal layer can vary quite a bit, even over the small sample size. A STEM picture of one of the vapor deposited aluminum samples shows that the material appeared to separate from the substrate during sample preparation (fig. 12). This seems consistent with the large variations in surface resistivity for those samples

discussed in the last section, which could be caused by flaking off of the metal from the substrate in some areas.

4. **Quality measurement conclusions.** While the samples were subjected to the stated quality measurements, the actual amount of material used for each test was a small portion of the sample size used for any of the electromagnetic tests. In fact, certain samples exhibit significant variation even by visual inspection. It also should be noted that the resistivities measured by the various materials do not agree with what would be predicted theoretically using Fuch's equation and the intended thicknesses. The resistivity measurements suggest the possibility that the metal thicknesses may be significantly higher than the intended values despite the results obtained from the STEM.

V. Results

The results from the measurements described in the previous sections are presented here. A plot is shown for each metal coating type in figures 13-16 (vapor deposited aluminum, sputtered aluminum, sputtered gold, and sputtered silver). On each plot, emissivity values are shown as a function of material thickness. The values for each measurement are connected with straight line segments and plotted with different line types to distinguish them. To demonstrate the range of variation of emissivity as a function of frequency for the L-band waveguide measurements, values of emissivity are shown at three different frequencies: at the low, high, and midpoint of the band. Also, Table 6 gives the emissivity values, number of tests, and standard deviations for the radiometer measurements.

Several trends can be observed by comparing the plots for the different materials. In general, as is expected, the emissivities decrease with material thickness. The measurement from the waveguide system and the free space system agree quite well, with the radiometer system generally giving a higher value for the emissivities than the other two systems. Also, the three different waveguide values for each thickness agree well, indicating that not much frequency variation occurs.

For the vapor deposited aluminum samples, it can be seen from figure 13 that the 100 Å sample demonstrated quite large emissivity values for all the measurement techniques. Even the 650 Å and 1500 Å samples had emissivities above 0.01 for all the techniques, and the 3000 Å emissivity was well above 0.01 as measured by the radiometer technique. The sputtered aluminum and gold samples shown in figures 14 and 15 give emissivities below 0.01 for both the 1500 Å and 3000 Å thicknesses for all but the radiometer technique, and the silver samples shown in figure 16 all have emissivity values below 0.01 for the sample thicknesses except for the radiometer technique.

VI. Conclusions

Some general conclusions can be drawn from the results presented in the last section. Overall, the silver samples showed the lowest values of emissivity, while vapor deposited aluminum showed the highest. This fact, coupled with the tendency of the vapor deposited aluminum to flake and peel from the substrate (seen in the electron microscope pictures of this material), tends to indicate that it is not acceptable for inflatable radiometer use.

The disagreement between the radiometer measurement system and the other techniques indicates that further investigation into the measurement of emissivities of metallic coated thin membranes is needed. The radiometer system gives a direct measurement of emissivity, while the other two techniques rely on computing emissivity indirectly from equations (1) or (12). However, there seems to be a wide variation in the values of emissivity measured by the radiometer system, which have to be averaged to obtain the final value. This wide variation, which is caused by the difficulty of accurate surface temperature measurements on the sample and the cold load, causes a high degree of uncertainty in the measurement (see Table 6). Also, a planned detailed error analysis for each technique has not yet been completed, but it will allow for more realistic direct comparison between the measurement techniques. A theoretical derivation of the emissivity for thin metallic films is also being conducted (ref. 2) which will provide another comparison. Further study is needed to determine which measurement of emissivity is the most correct. A future publication is planned with a more detailed error analysis, the planned S-band waveguide measurement results, and a comparison between theoretical and measured data.

VII. References

[1] Freeland, R. E.; Bilyeu, G. D.; and Veal, G. R.: Validation of a Unique Concept for a Low-Cost, Lightweight Space-Deployable Antenna Structure. IAF-93-I.1.204, October 1993.

[2] Prepared by Aerojet Electronic Systems Division: Critical Design Review for the Special Sensor Microwave Imager Sounder (SSMIS), Presented to the Department of the Air Force, Contract No. F04701-89-C-0036, June 4-6, 1991.

[3] Harrington, R. F.: Theoretical Analysis of the Emissivity of a Thin Metallic Membrane. Master contract agreement NAS1-19858, Task 44, January 1, 1994-March 31, 1995.

[4] Blume, H.-J. C.: Measurement Apparatus and Procedure for the Determination of Surface Emissivities. U. S. Patent 4,645,358, December 1985.

[5] HP8510C Network Analyzer Operating and Programming Manual, Hewlett-Packard Company,

[6] Dr. Koorosh Guidanean, Private Communication, L'Garde Inc., Tustin, California.

Acknowledgments

The authors would like to thank the following people for their work on this project: Patsy Tiemsin and Ken Dudley of NASA LaRC and Tim Overstreet and Kerri Bussell of Old Dominion University Research Foundation for work on the waveguide measurements, surface resistivity measurements, and microscope pictures; Don Oliver of NASA LaRC for the free-space sample holder construction; Dion Fralick of Lockheed Engineering and Sciences Company for assistance with the free-space measurements; Phil Bartley of Innovative Measurement Resources for free-space measurement software development; and Ann St. Clair of NASA LaRC for providing STEM pictures and other thickness measurements.

Thickness	AL VDA	AL Sputtered	AG Sputtered	AU Sputtered
100 Å	X			
600 Å	X	X	X	X
1500 Å	X	X	X	X
3000 Å	X	X	X	X

Table 1. Materials Used for Emissivity Measurements

Test	Emissivity
1	.01554906 *
2	.0403249
3	.0470598 *
4	.03477891
5	.03091518
6	.03611999
7	.02263838
8	.02088942 *
9	.03708775
10	.04194461

* Not included
Average Emissivity = .034829
Standard Deviation = .005995

Table 2. Emissivity values for 10 tests of 650 Å sputtered gold

Material		Silver (sputtered)	Gold (sputtered)	Aluminum (sputtered)	Aluminum (vapor deposited)
100 Å	Average value	-	-	-	**6.7604**
	Standard deviation	-	-	-	1.2281
	% error	-	-	-	18.166
650 Å	Average value	**0.7514**	**1.2279**	**1.9836**	**2.2613**
	Standard deviation	0.0496	0.0378	0.0853	1.8315
	% error	6.6087	3.0831	4.3019	80.994
1500 Å	Average value	**0.2608**	**0.5099**	**0.8683**	**2.2228**
	Standard deviation	0.0191	0.0031	0.0618	0.4942
	% error	7.3346	0.6124	7.1245	22.232
3000 Å	Average value	**0.1258**	**0.2594**	**0.8007**	**1.6623**
	Standard deviation	0.0064	0.0029	0.0834	1.4217
	% error	5.0991	1.1472	10.426	85.526

Table 3. Surface Resistivity Measurements (Ohms/square) - L'Garde

Material		Silver (sputtered)	Gold (sputtered)	Aluminum (sputtered)	Aluminum (vapor deposited)
100 Å	Average value	-	-	-	**5.377**
	Standard deviation	-	-	-	0.334
	% error	-	-	-	6.206
650 Å	Average value	**0.631**	**1.117**	**1.904**	**5.321**
	Standard deviation	0.019	0.001	0.078	0.403
	% error	2.953	0.127	4.106	7.574
1500 Å	Average value	**0.300**	**0.543**	**1.005**	**2.432**
	Standard deviation	0.011	0.001	0.068	0.086
	% error	3.621	0.244	6.745	3.557
3000 Å	Average value	**0.125**	**0.240**	**0.522**	**0.828**
	Standard deviation	0.008	0.002	0.014	0.025
	% error	6.215	0.857	2.657	3.054

Table 4. Surface Resistivity Measurements (Ohms/square) - LaRC

Material	Intended Thickness of Metal	Measured Thickness of Metal (Average)	% error
Silver, sputtered	650 Å	730 Å	12.3
	1500 Å	1586 Å	5.7
	3000 Å	3050 Å	1.7
Gold, sputtered	650 Å	671 Å	3.2
Aluminum, sputtered	650 Å	488 Å	-24.9

Table 5. Sample Thicknesses from STEM

Material	Emissivity (Average)	Number of Tests	Standard Deviation
Vapor Deposited 100 Å Al	.17261	9	.02471
Vapor Deposited 650 Å Al	.06629	10	.00861
Vapor Deposited 1500 Å Al	.02726	6	.00409
Vapor Deposited 3000 Å Al	.02830	9	.00667
Sputtered 650 Å Al	.03618	7	.00675
Sputtered 1500 Å Al	.02073	9	.00711
Sputtered 3000 Å Al	.03655	9	.00708
Sputtered 650 Å Au	.03483	7	.00600
Sputtered 1500 Å Au	.01560	8	.00940
Sputtered 3000 Å Au	--	--	--
Sputtered 650 Å Ag	.02414	8	.00481
Sputtered 1500 Å Ag	.01954	6	.00354
Sputtered 3000 Å Ag	-.00300	2	.00721

Table 6. Radiometric Emissivity Measurements

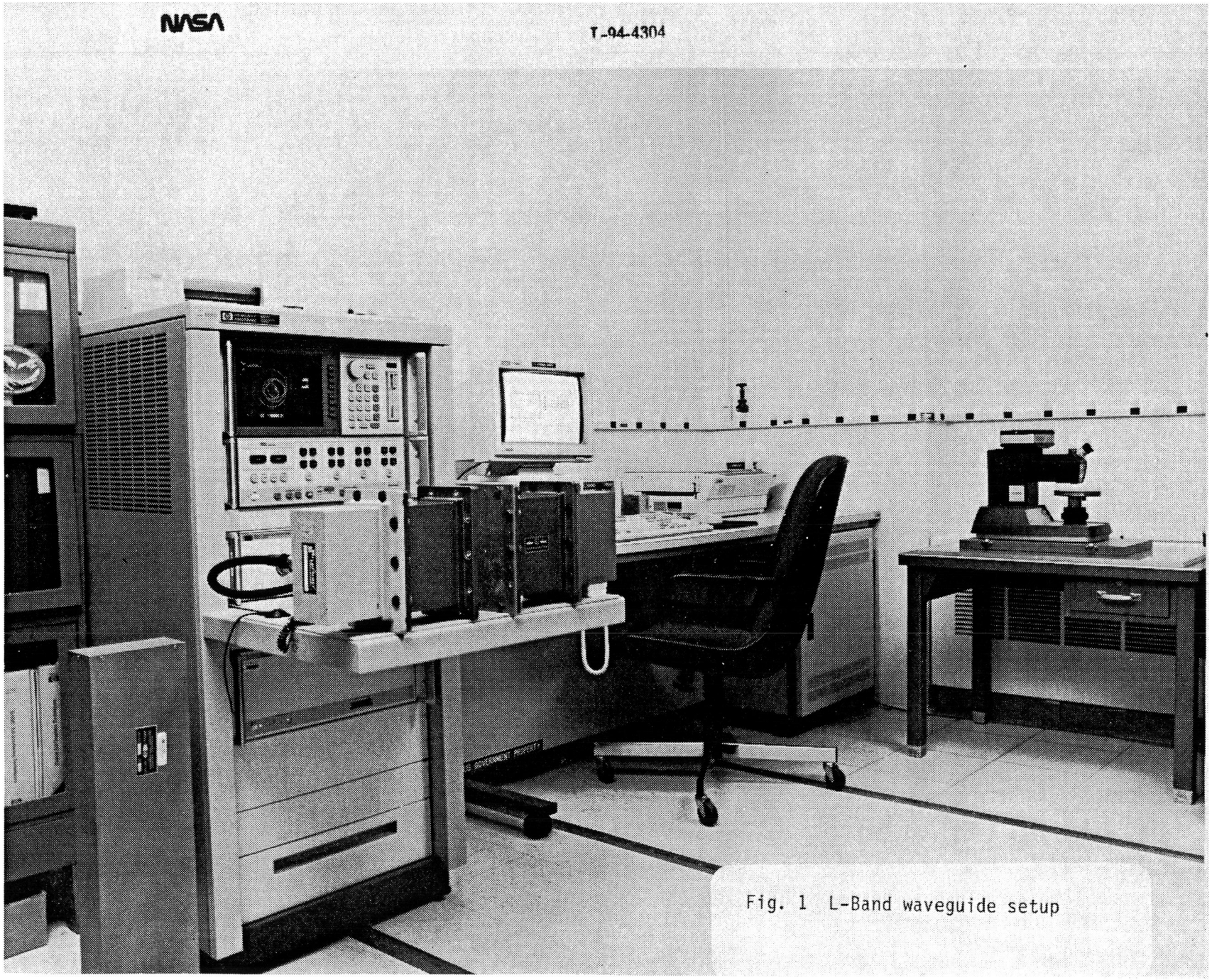

Fig. 1 L-Band waveguide setup

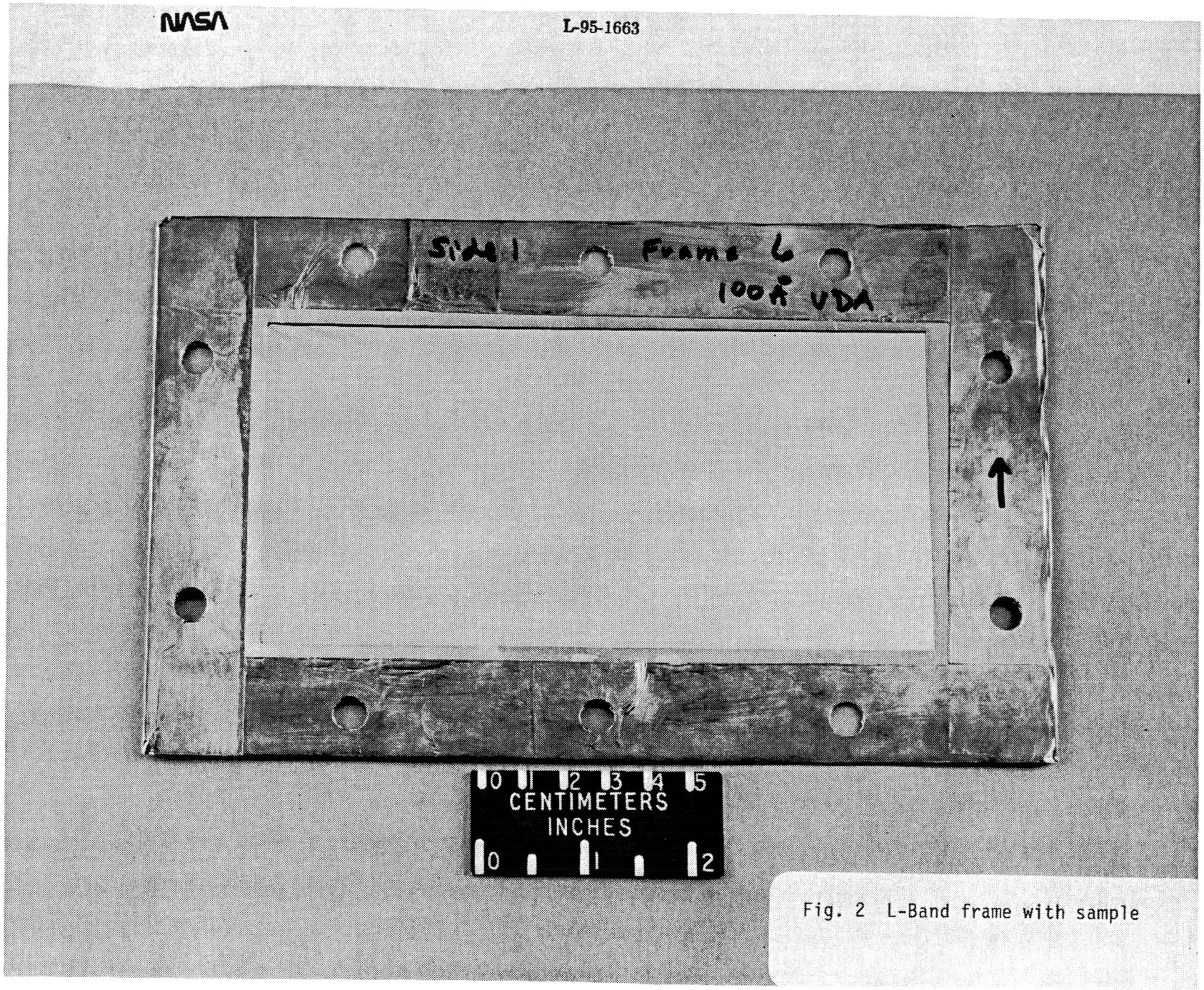

Fig. 2 L-Band frame with sample

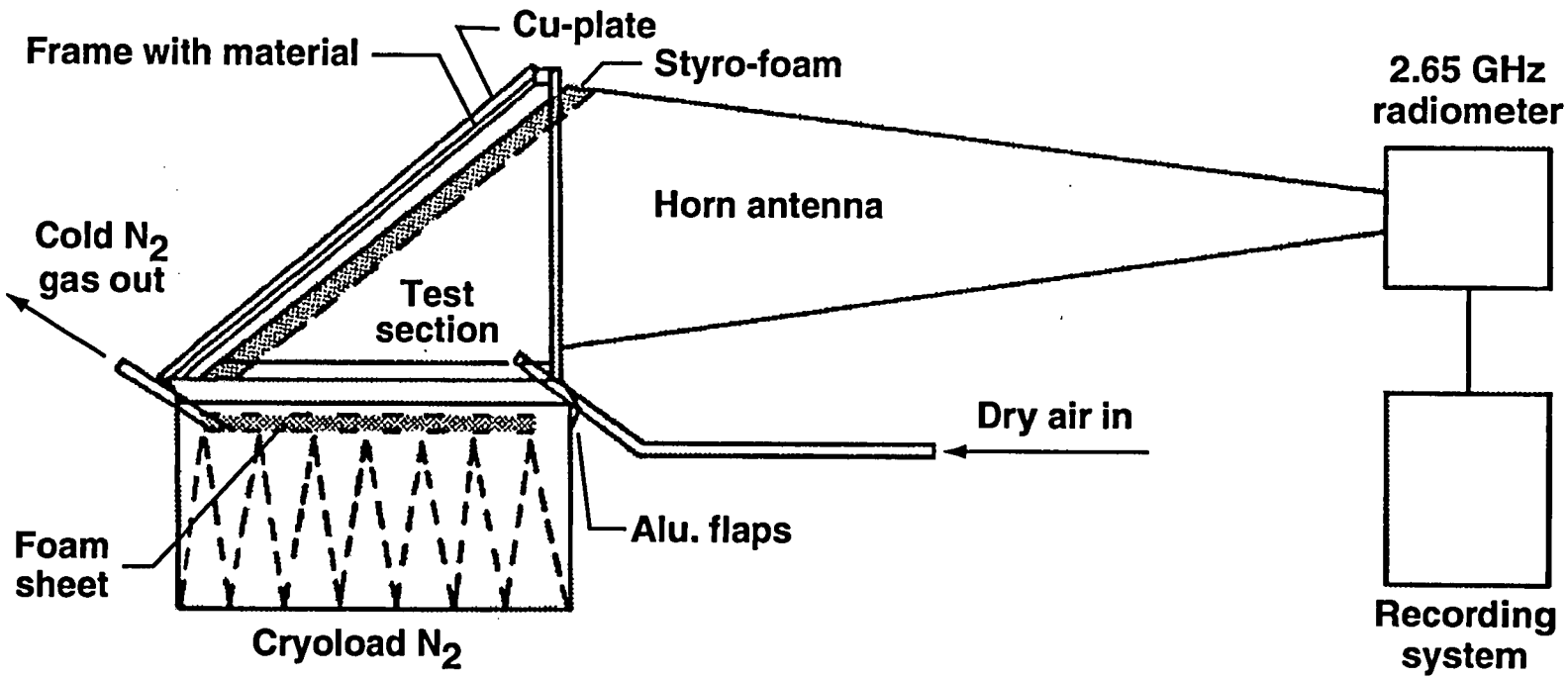

Fig. 3 Apparatus for measurements of Emissivity or intrinsic losses of surfaces of flat plates

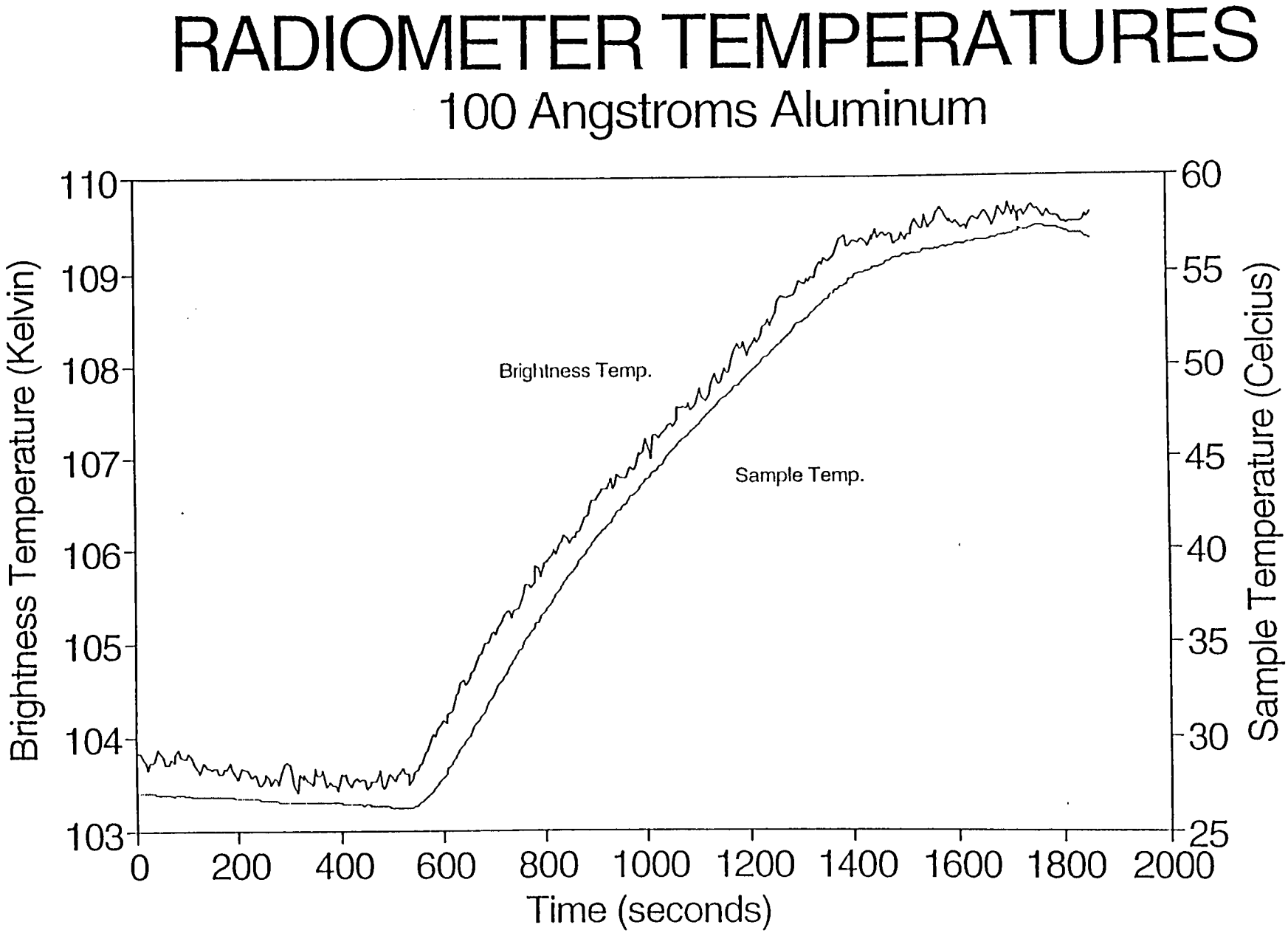

Fig. 4 Radiometer Temperatures during test of 100 Å Aluminum

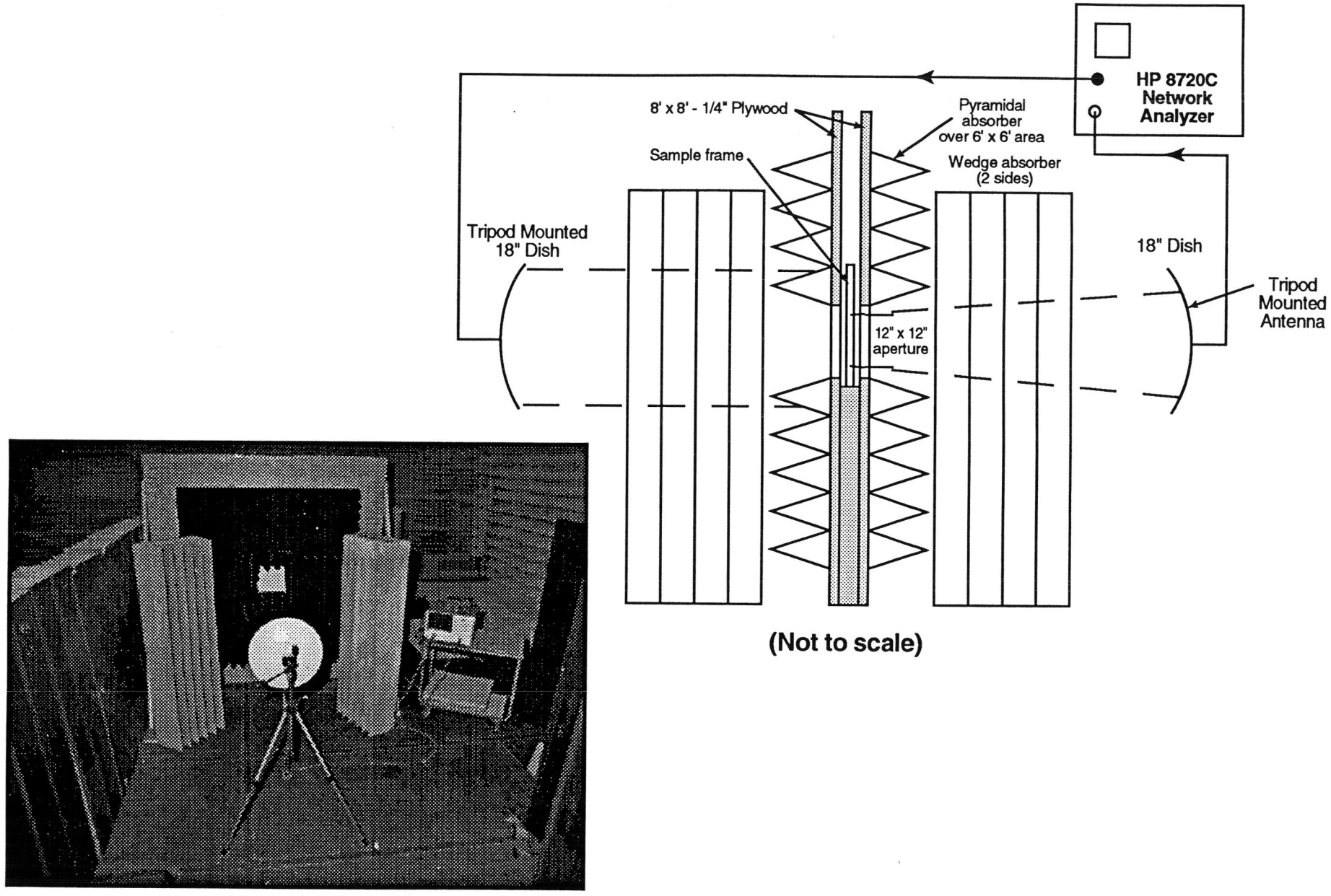

Fig. 5 C-Band Free Space Transmission System Concept

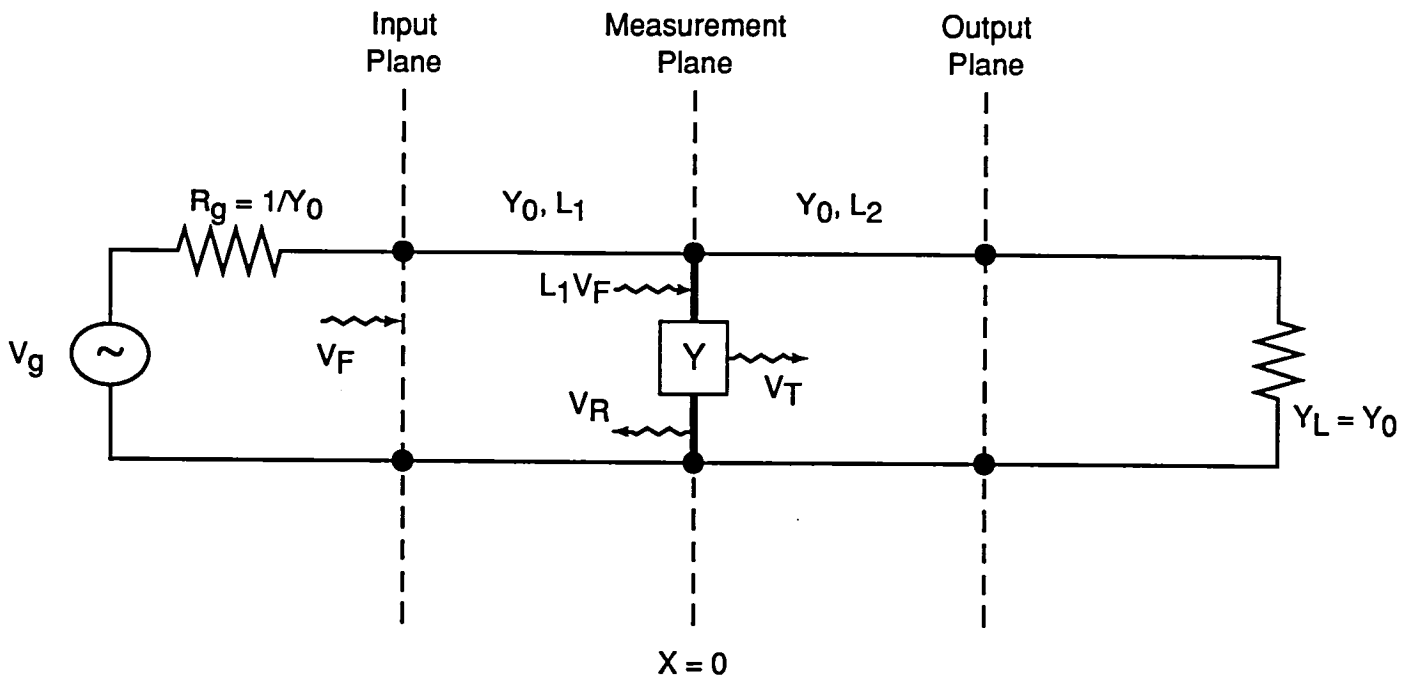

Fig. 6 Transmission line with lumped discontinuity model of test fixture

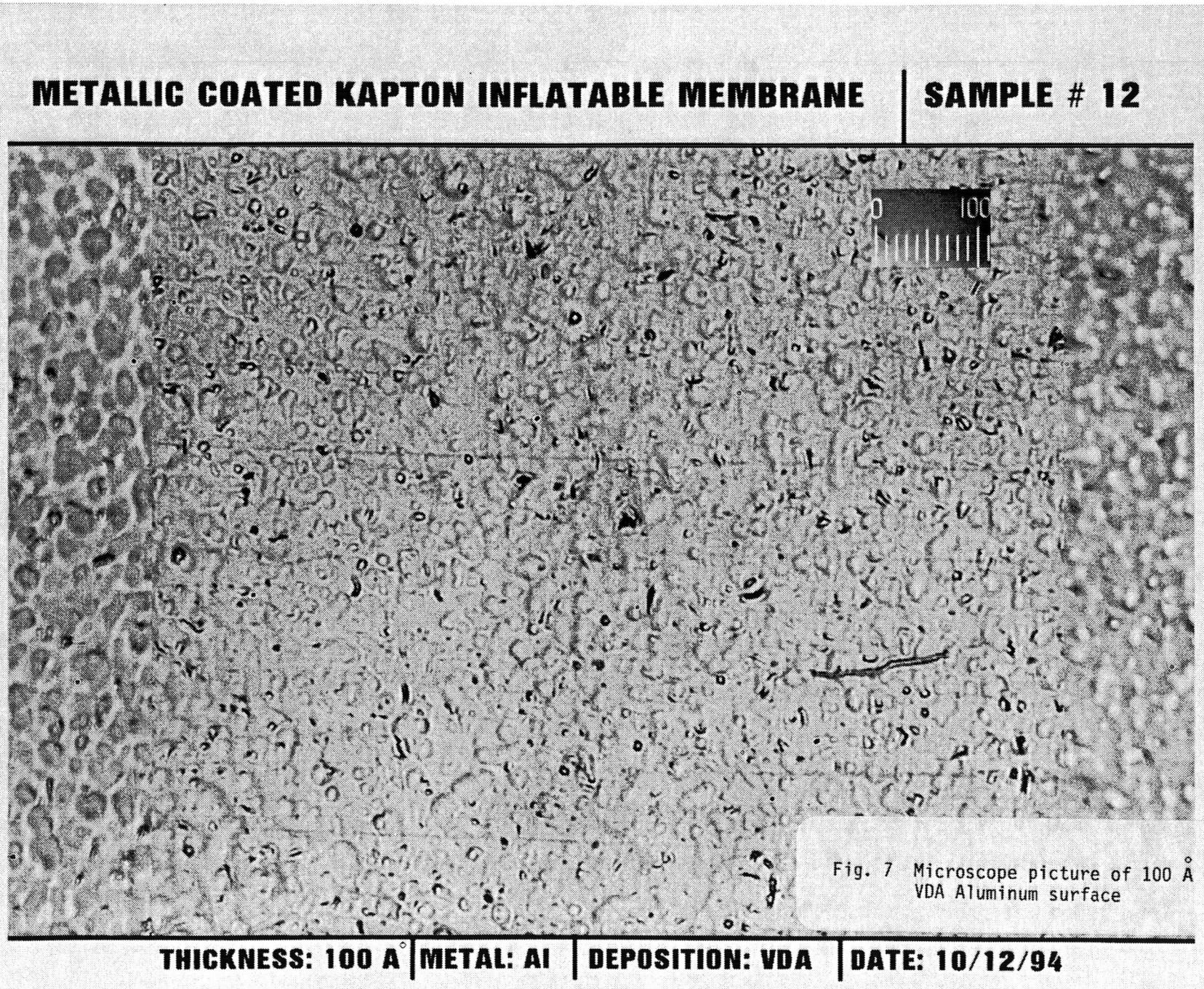

Fig. 7 Microscope picture of 100 Å VDA Aluminum surface

METALLIC COATED KAPTON INFLATABLE MEMBRANE | **SAMPLE # 5**

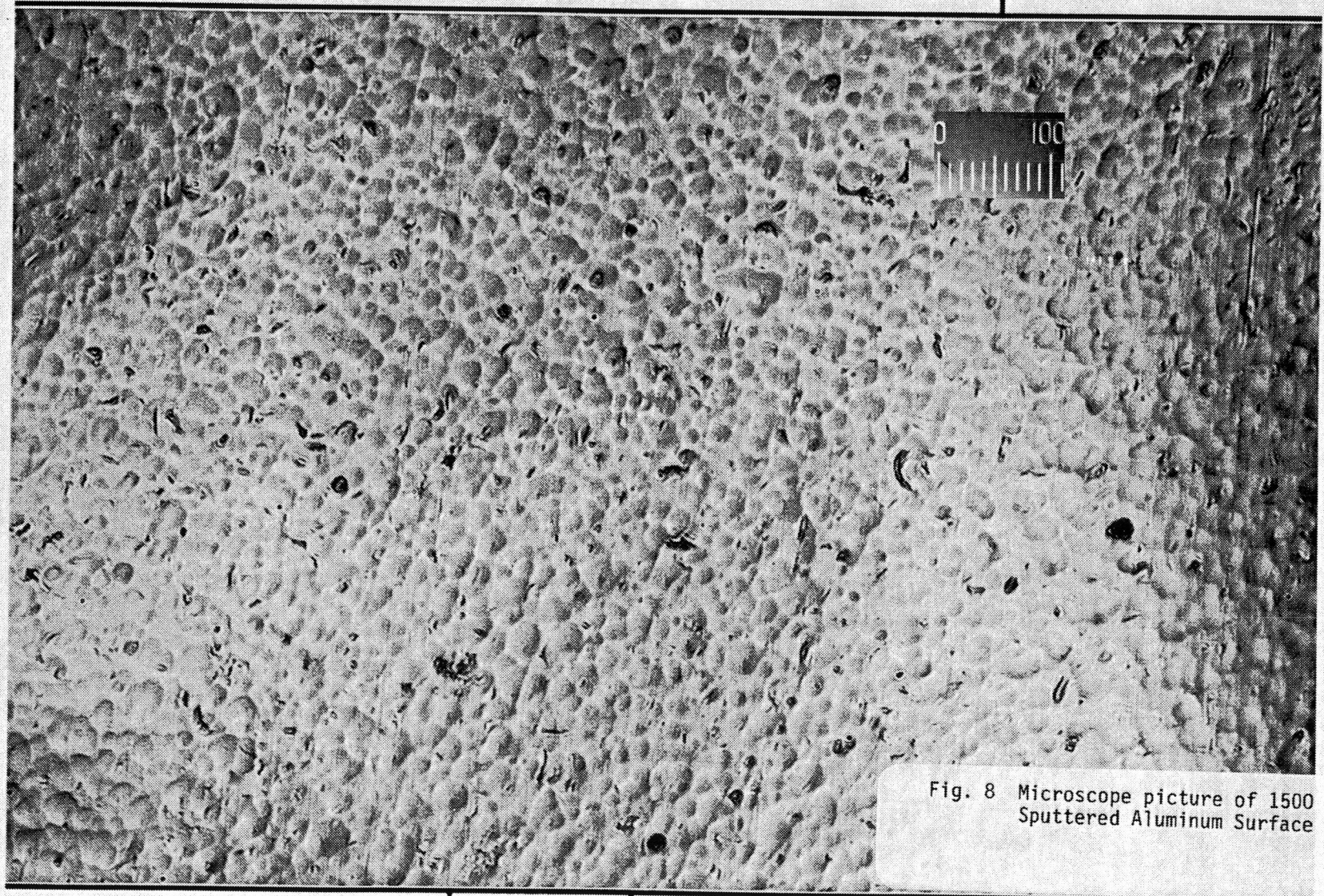

Fig. 8 Microscope picture of 1500 Å Sputtered Aluminum Surface

THICKNESS: 1500 A° | **METAL: Al** | **DEPOSITION: SPT** | **DATE: 10/12/94**

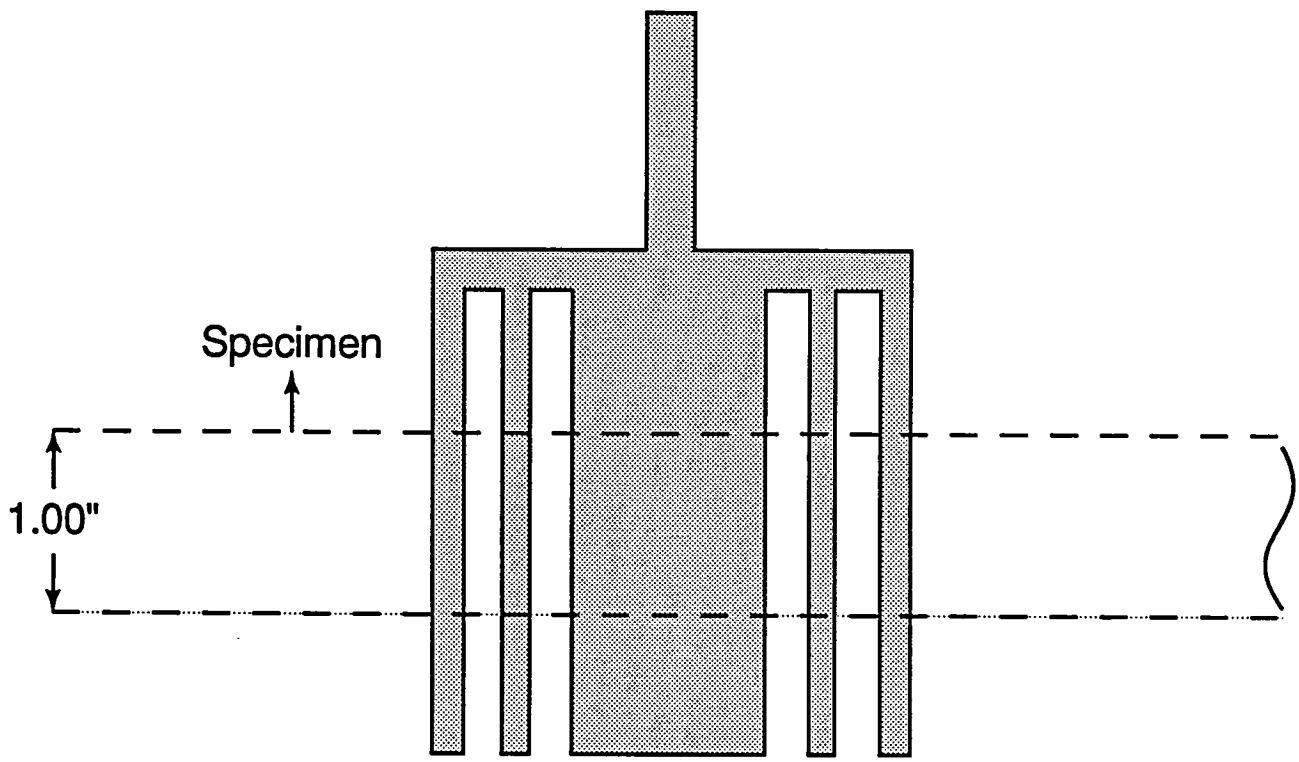

Fig. 9 Four-Probe Array for Surface Resistivity Measurements

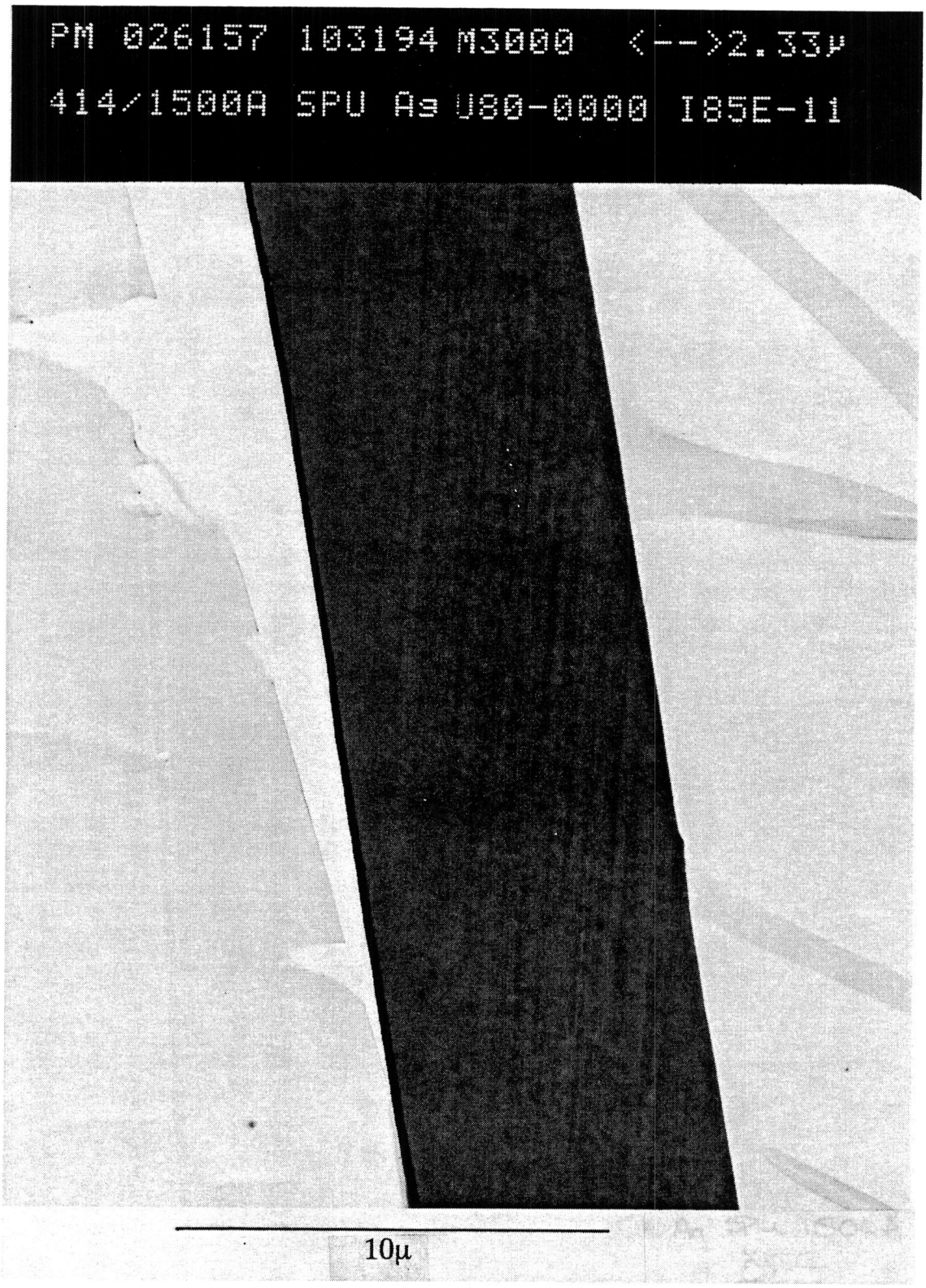

Fig. 10 STEM picture of 1500 Å sputtered silver cross section

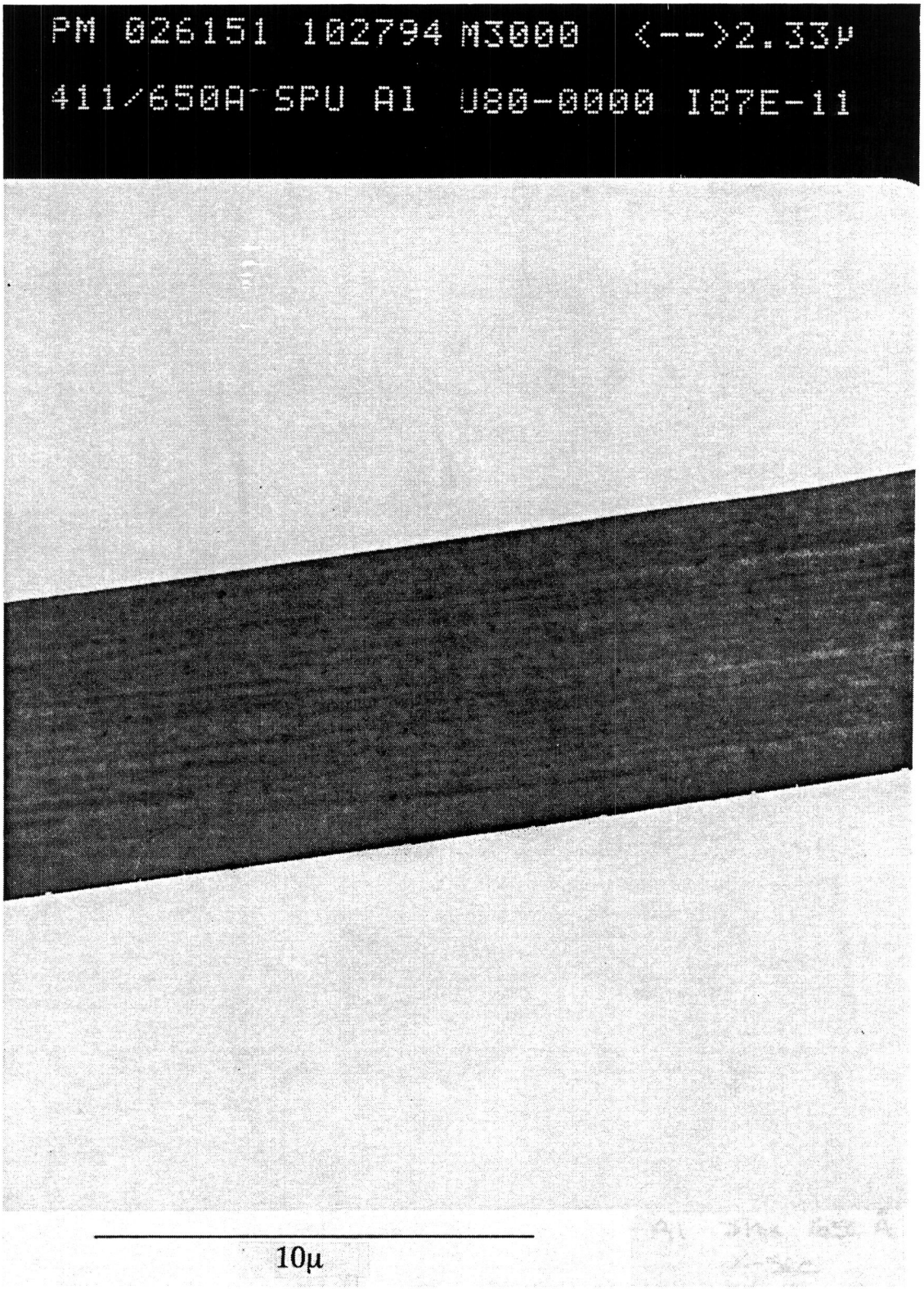

Fig. 11 STEM picture of 650 Å sputtered aluminum cross section

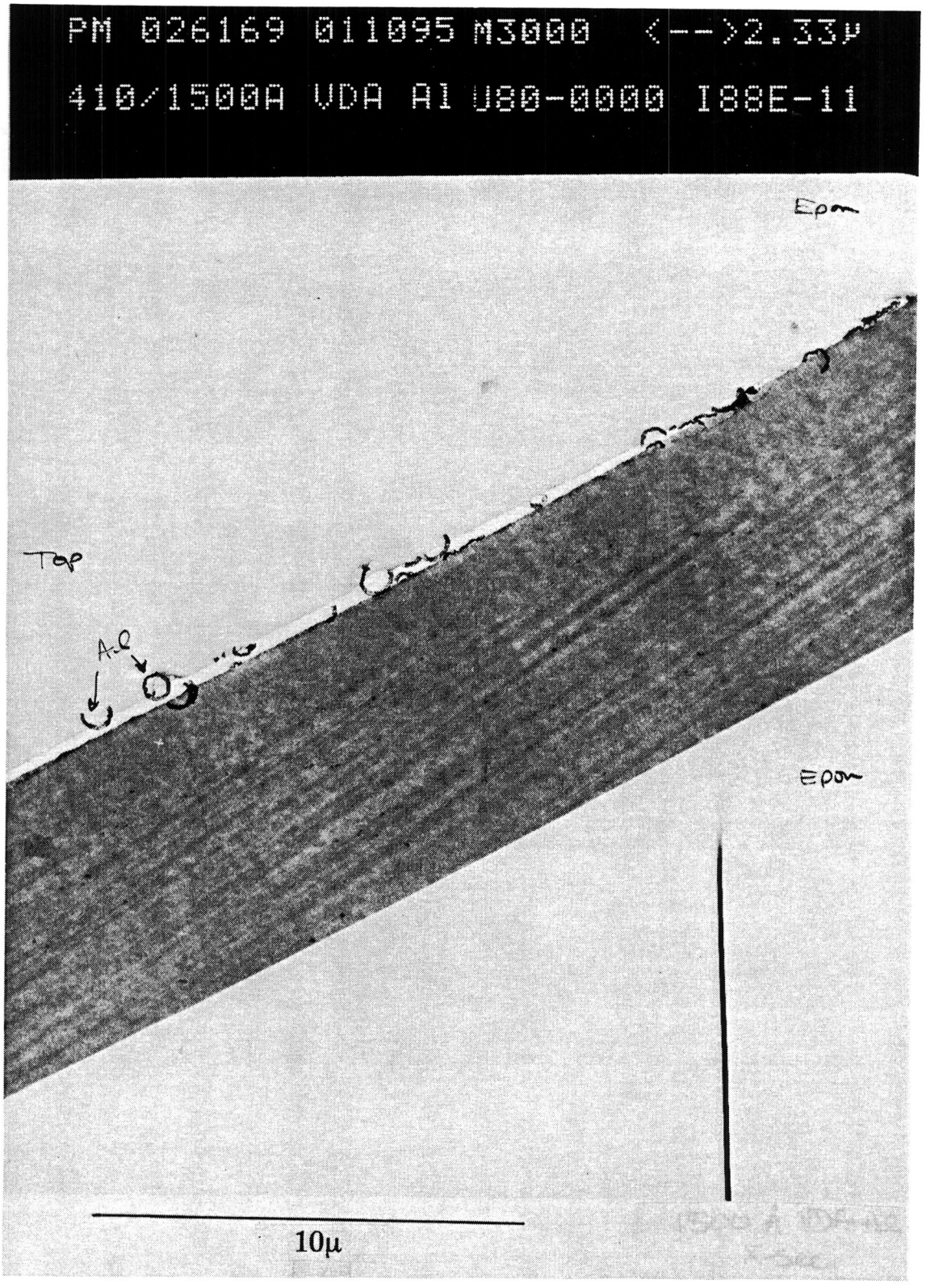

Fig. 12 STEM picture of 1500 Å VDA aluminum cross section

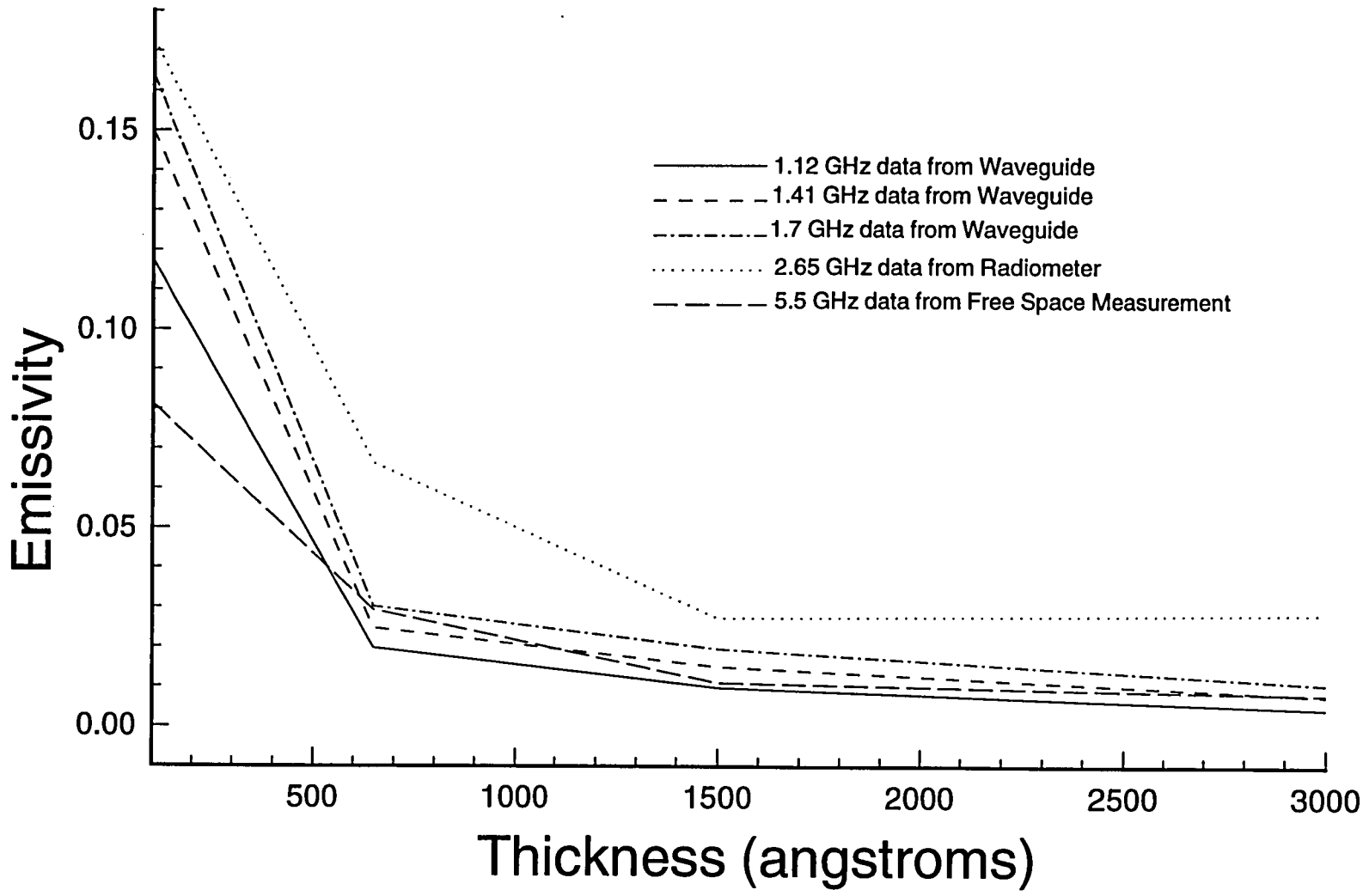

Fig. 13 Plot of emissivity as a function of metal thickness for Vapor Deposited Aluminum

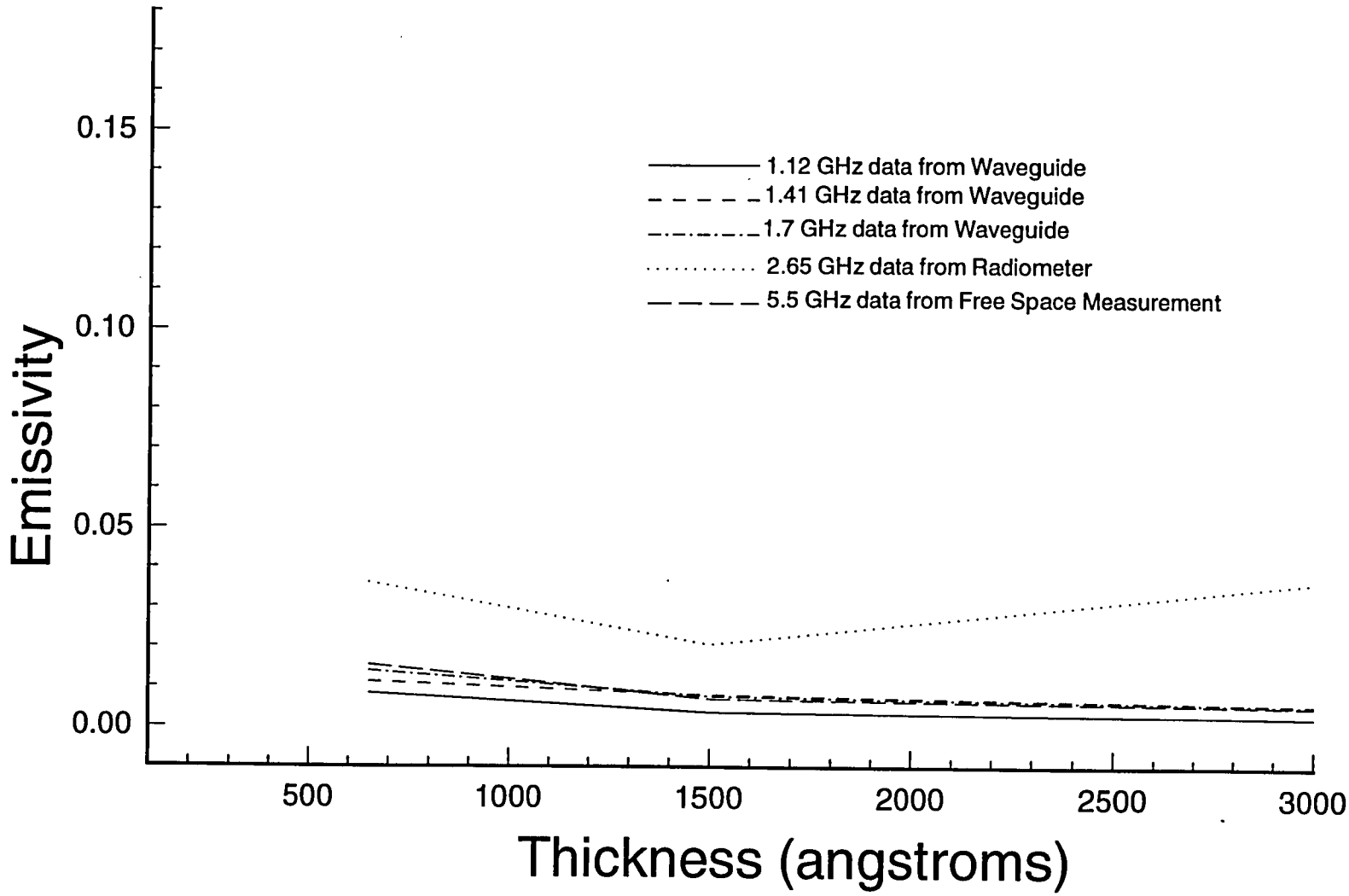

Fig. 14 Plot of emissivity as a function of metal thickness for sputtered Aluminum

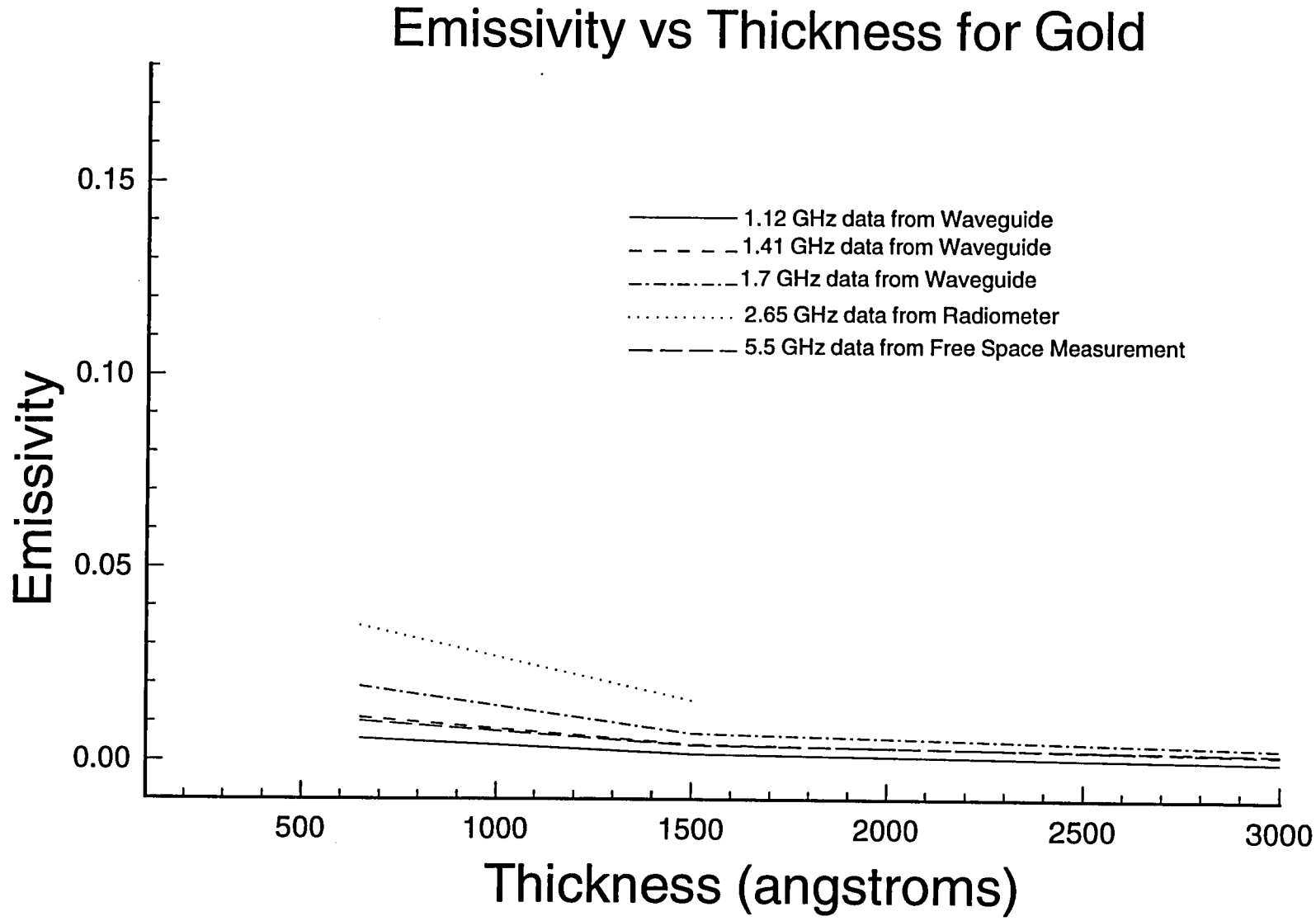

Fig. 15 Plot of emissivity as a function of metal thickness for Gold

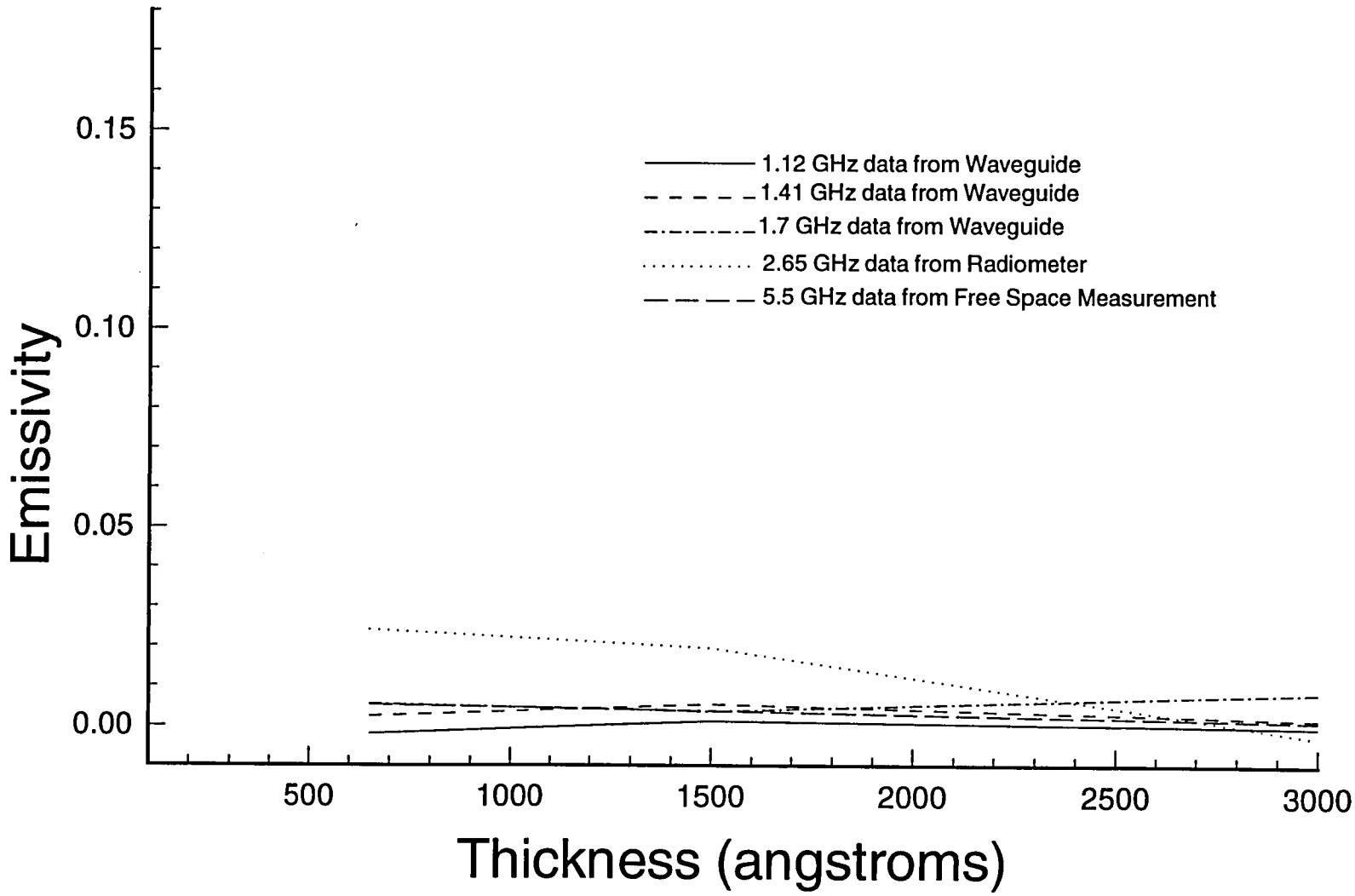

Fig. 16 Plot of emissivity as a function of metal thickness for Silver

REPORT DOCUMENTATION PAGE

Form Approved
OMB No. 0704-0188

1. AGENCY USE ONLY *(Leave blank)*	2. REPORT DATE	3. REPORT TYPE AND DATES COVERED
	June 1995	Technical Memorandum

4. TITLE AND SUBTITLE
Emissivity Measurements in Thin Metallized Membrane Reflectors Used for Microwave Radiometer Sensors

5. FUNDING NUMBERS
WU 233-01-03-06

6. AUTHOR(S)
Lyle C. Schroeder, Robin L. Cravey, Michael J. Scherner, Chase P. Hearn, and Hans-Juergen C. Blume

7. PERFORMING ORGANIZATION NAME(S) AND ADDRESS(ES)
NASA Langley Research Center
Hampton, VA 23681-0001

8. PERFORMING ORGANIZATION REPORT NUMBER

9. SPONSORING / MONITORING AGENCY NAME(S) AND ADDRESS(ES)
National Aeronautics and Space Administration
Washington, DC 20546-0001

10. SPONSORING / MONITORING AGENCY REPORT NUMBER
NASA TM-110179

11. SUPPLEMENTARY NOTES

12a. DISTRIBUTION / AVAILABILITY STATEMENT
Unclassified - Unlimited

Subject Category 17

12b. DISTRIBUTION CODE

13. ABSTRACT *(Maximum 200 words)*

This paper is concerned with electromagnetic losses in metallized films used for inflatable reflectors. An inflatable membrane is made of tough elastic material such as Kapton, and it is not electromagnetically reflective by design. A film of conducting metal is added to the membrane to enhance its reflective properties. Since the impetus for use of inflatables for spacecraft is the light weight and compact packaging, it is important that the metal film be as thin as possible. However, if the material is not conductive or thick enough, the radiation due to the emissivity of the reflector could be a significant part of the radiation gathered by the radiometer. The emissivity would be of little consequence to a radar or solar collector; but for a radiometer whose signal is composed of thermal radiation, this contribution could be severe. Bulk properties of the metal film cannot be used to predict its loss. For this reason, a program of analysis and measurement was undertaken to determine the emissivities of a number of candidate metallized film reflectors. This paper describes the three types of measurements which were performed on the metallized thin films: (1) a network analyzer system with an L-band waveguide, (2) an S-band radiometer, and (3) a network analyzer system with a C-band antenna free-space transmission system.

14. SUBJECT TERMS	15. NUMBER OF PAGES
radiometer, metallized thin film, inflatable, emissivity	41
	16. PRICE CODE: A03

17. SECURITY CLASSIFICATION OF REPORT	18. SECURITY CLASSIFICATION OF THIS PAGE	19. SECURITY CLASSIFICATION OF ABSTRACT	20. LIMITATION OF ABSTRACT
Unclassified	Unclassified		